JOURNAL OF PHYSICAL ORGANIC CHEMISTRY, VOL. 9, 79–86 (1996)

GAS-PHASE (ION CYCLOTRON RESONANCE SPECTROMETRIC) AND SOLID-STATE (CRYSTALLOGRAPHIC) STUDIES OF HIGHLY SUBSTITUTED PYRAZOLES

JOSE-LUIS M. ABBOUD, CONCEPCION FOCES-FOCES,* MARTA HERREROS, HAMID HOMAN,
LOURDES INFANTES AND RAFAEL NOTARIO*
Departamento de Cristalografía e Instituto de Química Física 'Rocasolano,' CSIC, Serrano 119, E-28006 Madrid, Spain
ADOLF W. KREBS* AND JÖRG NEUBAUER
Institut für Organische Chemie, Universität Hamburg, Martin-Luther-King-Platz 6, D-20146 Hamburg, Germany
AND
JOSÉ ELGUERO AND NADINE JAGEROVIC
Instituto de Química Médica, CSIC, Juan de la Cierva 3, E-28006 Madrid, Spain

The gas-phase basicities of 3,4,5-tri-*tert*-butylpyrazole (I) and 1,3,4,5-tetra-*tert*-butyl-pyrazole (II) were measured by Fourier transform ion cyclotron resonance spectrometry. The x-ray molecular structures of I·HCl (a monohydrate) and II were determined. A clear lack of planarity is present in the pyrazole rings because of the steric effects of the *tert*-butyl substituents. The C_{sp^3} atom bonded to N-1, C-3, C-4 and C-5 atoms deviates significantly from the pyrazole plane, as expected on the basis of semi-empirical AM1 calculations. In I·HCl, the molecules form dimers through symmetry centres in which the chlorine atom and the water molecules play an important role.

INTRODUCTION

The structure and physico-chemical properties of distorted aromatic compounds (either in-plane[1] or out-of-plane deformations)[2] are of interest. The distortion is usually achieved by paracyclophane bridging[3,4] or by steric congestion.[5] The situation is common in six-membered rings, such as benzenes, but much more infrequent in five-membered heteroaromatic rings.[6] Since the hindered pyrazoles I and II had been prepared in previous work,[6] it was decided to study their gas-phase basicity and their solid-state geometry. In this respect, we recall that experimental studies have been performed on the kinetics of proton exchange between unhindered or moderately hindered n-bases and 1,3,5-tri(*tert*-butyl)benzene or 3,5-di(*tert*-butyl)toluene[7] and 2,6-di(*tert*-butyl)pyridine.[8] Here, attention was focused primarily on the potential thermodynamic effects of steric hindrance.

EXPERIMENTAL

FT-ICR. The gas-phase basicity (*GB*) of a base B is defined as the standard Gibbs energy change for the reaction

$$\begin{gathered} BH^+(g) \rightarrow B(g) + H^+(g) \\ GB(B) = \Delta G_{H^+}(g) \end{gathered} \qquad (1)$$

The proton affinity (*PA*) is defined as $PA(B) = \Delta H_{H^+}(g)$.

*GB*s were determined from equilibrium proton-transfer reactions conducted in a modified Bruker CMS-47 Fourier transform ion cyclotron resonance (FT-ICR)[9] mass spectrometer used in previous studies.[10] Its high magnetic field strength (4·7 T) easily allows the

---

* Authors for correspondence.

CCC 0894–3230/96/020079–08

Received 24 July 1995
Revised 25 September 1995

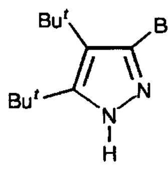

I

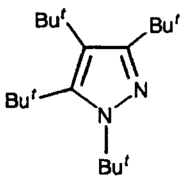

II

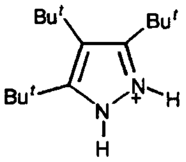

IH⁺

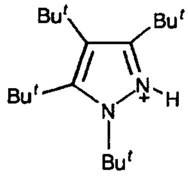

IIH⁺

monitoring of proton exchange reactions for relatively long periods of time.

Table 1 presents the results of proton-transfer equilibria (2) obtained in this study along with the standard bases used (B_{ref}).

$$B_{ref}H^+(g) + \mathbf{I}\ (\text{or } \mathbf{II})(g) \rightleftharpoons \mathbf{IH}^+\ (\text{or } \mathbf{IIH}^+)(g) + B_{ref}(g) \qquad K_P,\ \delta\Delta G_{H^+}(g) \quad (2)$$

The relevant ions, $B_{ref}H^+(g)$, $\mathbf{IH}^+(g)$ and $\mathbf{IIH}^+(g)$, were generated by chemical ionization. Gaseous mixtures of **I** or **II** and the corresponding reference bases were ionized by electron impact (nominal ionization energies in the range 11–13 eV). The reactive fragment ions thus formed acted as proton sources. For each equilibrium, K_P values are the average of at least six different measurements, carried out on mixtures having different total pressures. Also, the ratios of the reagents were varied as much as possible. Reaction times were generally 10–15 s. In every case, double-resonance-like experiments were performed. Thus, $\mathbf{IH}^+(g)$ [or $\mathbf{IIH}^+(g)$] was isolated by ejecting all other ions by means of radiofrequency 'chirps' (broad-band mode) and proton transfer was allowed to take place. The signal of $B_{ref}H^+(g)$ appeared, grew and finally levelled off after reaction times of 5–10 s. At these times and beyond, the ratio of the relevant ion intensities agreed well with the values obtained in standard equilibration runs. Similar experiments were performed in which $B_{ref}H^+$ was isolated. Their outcome was the same.

The reversibility of reaction (2) was confirmed by means of double-resonance experiments. The values of $\delta\Delta G_{H^+}(g)$ given in Table 1 are defined as $\delta\Delta G_{H^+}(g) = -RT \ln K_P$. All *GB*s are referred to ammonia (the gas-phase basicities of the reference compounds are published values from Taft's laboratory;[11a] they have been anchored to the most recent high-pressure mass spectrometric work by Szulejko and McMahon[11b] as indicated in Ref. 10b. Thus, with respect to this reference, $GB(B) = -\Delta\Delta G_{H^+}(g)$ for the reaction

$$\mathbf{I}\ (\text{or } \mathbf{II})(g) + NH_{4^+}(g) \rightleftharpoons \mathbf{IH}^+\ (\text{or } \mathbf{IIH}^+)(g) + NH_3(g) \qquad \Delta\Delta G_{H^+}(g) \quad (3)$$

$\Delta\Delta G_{H^+}(g)$ is the average of the $\Delta\Delta G$ values obtained through the equation

$$\Delta\Delta G = \delta\Delta G_{H^+}(g) + \Delta\Delta G_{H^+}(\text{std}) \qquad (4)$$

where $\Delta\Delta G_{H^+}(\text{std})$ pertains to the reaction

$$B_{ref}(g) + NH_{4^+}(g) \rightleftharpoons B_{ref}H^+(g) + NH_3(g) \qquad (5)$$

The corresponding *PA* values relative to ammonia and presented in Table 5 were obtained using entropy changes $\Delta\Delta S$ estimated by means of the appropriate changes in symmetry numbers as described in Ref. 12.

X-ray structure determination. A summary of crystal data and refinement parameters is given in Table 2. The crystal of **II** was sealed in a glass capillary to prevent air decomposition. The structure of **IH⁺** was solved by Patterson and subsequent Fourier synthesis, while that of **II** was solved by direct methods (SIR92)[13] in the *Cc* space group. Since the molecule presents an almost binary axis passing through the N-2 atom and the mid-point of C-4–C-5, the refinements were carried out in the *Cc* and *C2/c* space groups. The *C2/c* group was chosen because of high values of the correlation parameters in *Cc* and unreliable bond distances and angles. Owing to the lack of symmetry in the pyrazole, a statistical disorder of 50% was assumed for the molecule. The refinements were carried out by least-squares procedures using full matrix. After several cycles of isotropic refinement in **IH⁺**, the $\Delta\rho$ map showed peaks that were assigned to the methyl groups of two *tert*-butyl groups. These peaks were then refined

Table 1. Gas-phase basicities of pyrazoles **I** and **II** obtained with reference bases (all values in kcal mol^{-1})

Compound	Reference base	$\Delta\Delta G_{H^+}$(std)	$\delta\Delta G_{H^+}$(g)	$\Delta\Delta G$	$\Delta\Delta G_{H^+}$(g)
3,4,5-Tri-*tert*-butylpyrazole (**I**)	$EtNMe_2$	−26·0	−1·60	−27·60	−27·7 ± 0·1
	Pr^i_2NH	−28·2	0·35	−27·85	
1,3,4,5-Tetra-*tert*-butylpyrazole (**II**)	Et_3N	−31·3	−2·50	−33·80	−34·0 ± 0·2
	Pr^n_3N	−33·4	−0·82	−34·22	

with occupancy factors of 50/50 and 47/53 for the methyl groups bonded to C-6 and C-10, respectively. In spite of the high thermal factors of the other *tert*-butyl group, no disorder model could be obtained. Hydrogen atoms were located on a difference Fourier map, except some of the *tert*-butyl groups in **IH**$^+$, that were introduced at the calculated positions with respect to the observed positions. All hydrogen atoms in **II** were refined isotropically while only H-1, H-2, H-181 and H-182 were refined in **IH**$^+$. The scattering factors were taken from the *International Tables for X-Ray Crystallography*.[14] Table 3 lists the final atomic coordinates and equivalent thermal factors for non-hydrogen atoms. The calculations were carried out with the XTAL,[15] PESOS[16] and PARST[17] set of programs running on a VAX 6410 computer.

RESULTS AND DISCUSSION

The geometrical characteristics describing the molecular and crystal structures of **IH**$^+$ and **II** are given in Table 4. The atom numbering follows the scheme indicated in Figures 1 and 2.

The pyrazole ring is non-planar, especially in **II** ($\chi^2 = 32{\cdot}75$ and 1794·38 for **IH**$^+$ and **II**, respectively, vs the tabulated value of 5·99), owing to the steric

Table 2. Crystal analysis parameters at 200 K

Crystal data	**IH**$^+$	**II**
Formula	$C_{15}H_{29}N_2^+\cdot Cl^-\cdot H_2O$	$C_{19}H_{36}N_2$
Crystal habit	Colourless plate	Colourless plate
Crystal size (mm)	0·47 × 0·33 × 0·10	0·50 × 0·40 × 0·27
Symmetry	Monoclinic, $P2_1/c$	Monoclinic, $C2/c$
Unit cell determination	Least-squares fit from 49 reflections ($\theta < 45°$	Least-squares fit from 62 reflections ($\theta < 45°$)
Unit cell dimensions (Å, °)	a = 9·8843(10)	a = 17·8882(17)
	b = 16·7720(14)	b = 9·0100(6)
	c = 11·3002(15)	c = 12·0055(9)
	90, 112·08(1), 90	90, 104·256(7), 90
Packing: V (Å^3), Z	1736·0(3), 4	1875·4(2), 4
D_c (g cm^{-3}), M, F(000)	1·113, 290·88, 640	1·036, 292·51, 656
μ (cm^{-1})	19·21	4·17
Experimental data		
Technique	Four-circle diffractometer: Philips PW1100, bisecting geometry. Graphite oriented monochromator. $\omega/2\theta$ scans. Detector apertures 1 × 1°. 1 min/reflex.	
Radiation	Cu Kα	Cu Kα
Scan width	1·5°	1·5°
θ_{max}	65°	65°
Number of reflections:		
Independent	2971	1601
Observed	2521 [2σ(I) criterion]	1350 [2σ(I) criterion]
Standard reflections	2 reflections every 90 minutes	
	1·4% decay	1·5% decay
Solution and refinement:		
Solution	Patterson and difference synthesis	Direct methods: Sir92
Refinement: least-squares on F_o	Full matrix	
Parameters:		
Number of variables	243[a]	169
Degrees of freedom	2278	1181
Ratio of freedom	10·37	7·99
Final shift/error	0·13	0·01
Secondary extinction (/10^3)	3(1)	7(1)
H atoms	—[a]	From difference synthesis
Weighting scheme	Empirical so as to give no trends in $\langle \omega\Delta^2F\rangle$ vs $\langle \lvert F_{obs}\rvert \rangle$ and $\langle \sin\theta/\lambda\rangle$	
Max. thermal value (Å^2)	U33 [C(17)] = 0·27(1)	U11 [C(11)] = 0·082(2)
Final ΔF peaks (e Å^{-3})	0·52	0·34
Final R and R_w	0·084, 0·102	0·047, 0·059

[a] See Experimental.

Table 3. Atomic coordinates and equivalent thermal factors

Compound	Atom	x	y	z	U_{eq}	Atom	x	y	z	U_{eq}
I	Cl	−0·1216(1)	0·07935(6)	0·1124(1)	0·0701(5)	N-1	0·2282(3)	0·1600(2)	0·1075(3)	0·042(1)
	N-2	0·1144(3)	0·2012(2)	0·1129(3)	0·044(1)	C-3	0·1327(3)	0·2787(2)	0·1025(3)	0·041(1)
	C-4	0·2678(3)	0·2889(2)	0·0870(3)	0·039(1)	C-5	0·3263(3)	0·2109(2)	0·0935(3)	0·038(1)
	C-6	0·0100(4)	0·3318(2)	0·1132(6)	0·076(2)	C-71[a]	0·076(2)	0·4100(8)	0·196(2)	0·080(5)
	C-81[a]	−0·031(1)	0·2886(6)	0·231(1)	0·078(4)	C-91[a]	−0·114(1)	0·3414(9)	0·006(1)	0·095(5)
	C-72[a]	−0·1321(9)	0·2775(6)	0·071(2)	0·102(6)	C-82[a]	−0·050(1)	0·3847(6)	−0·031(1)	0·089(5)
	C-92[a]	0·036(2)	0·376(1)	0·219(2)	0·112(8)	C-10	0·3314(5)	0·3682(2)	0·0589(5)	0·072(2)
	C-111[b]	0·5121(8)	0·3687(5)	0·1396(8)	0·064(3)	C-121[b]	0·301(1)	0·4406(5)	0·139(1)	0·079(4)
	C-131[b]	0·299(1)	0·3840(6)	−0·0702(8)	0·077(4)	C-112[c]	0·178(1)	0·4110(6)	−0·058(1)	0·080(4)
	C-122[c]	0·400(2)	0·4190(7)	0·147(1)	0·088(6)	C-132[c]	0·404(1)	0·3497(7)	−0·046(1)	0·080(5)
	C14	0·4659(3)	0·1712(2)	0·0927(3)	0·048(1)	C-15	0·5963(4)	0·1974(6)	0·2062(5)	0·116(3)
	C-16	0·4901(5)	0·1848(5)	−0·0303(5)	0·101(3)	C-17	0·4536(7)	0·0818(4)	0·101(1)	0·130(5)
	O-18	0·1817(4)	0·0053(2)	0·1479(4)	0·066(2)					
II	N-1[a]	0·44471(8)	0·4562(2)	0·6878(1)	0·0390(5)	N-2	0·5	0·5424(2)	0·75	0·0483(7)
	C-3[a]	0·44471(8)	0·4562(2)	0·6878(1)	0·0390(5)	C-5	0·46256(9)	0·3053(2)	0·7131(1)	0·0361(5)
	C-6	0·38686(9)	0·5464(2)	0·5984(1)	0·0445(6)	C-7	0·4016(1)	0·1789(2)	0·6898(2)	0·0485(6)
	C-8	0·3247(1)	0·6110(3)	0·6518(2)	0·0641(8)	C-9	0·3521(1)	0·4622(3)	0·4871(2)	0·0589(7)
	C-10	0·4298(1)	0·6778(3)	0·5621(2)	0·0649(8)	C-11	0·4179(2)	0·0622(2)	0·7866(2)	0·0617(8)
	C-12	0·3231(1)	0·2418(3)	0·6974(2)	0·0610(8)	C-13	0·3925(2)	0·1007(2)	0·5733(2)	0·0617(8)

[a] Population parameter (pp) = 50%.
[b] pp = 53%.
[c] pp = 47%.

effect of contiguous *tert*-butyl groups. Moreover, angular distortions at the external angles of the aromatic carbon atom where the substituent is bonded are also observed: C–C-3–C-4 > C–C-3–N-2, and so on. The conformation of the pyrazole in IH^+ is a distorted envelope flapping at C-4 while II displays a half-chair conformation with C-4 and C-5 atoms lying above and below the plane defined by the other three. The Cremer and Pople parameters[18] for both rings are $q_2 = 0{\cdot}017(3)$ and 0·066(2) Å and $\Phi_2 = 113$ and 126°, respectively (vs 108 and 126° for the ideal envelope and half-chair conformations). In addition, the C_{sp^3}–C(pyrazole) bond appears to be elongated [1·534(5)–1·555(6) Å] in IH^+ and 1·554(2) in II, with respect to the mean value retrieved from the Cambridge Structural Database of 1·527(16) Å.[19] The other distance of 1·529(2) Å, in II, corresponds to the N/C–C_{sp^3} bonds owing to the statistical disorder (see Experimental). The C_{sp^3} atoms bonded to the pyrazole ring deviate from the mean-square pyrazole planes (Figures 3 and 4) up to 0·134(6) and 0·501(2) Å, respectively. The deformation increases with increasing number of contiguous *tert*-butyl substituents to alleviate the congestion of the methyl groups. When the *tert*-butyl groups are further

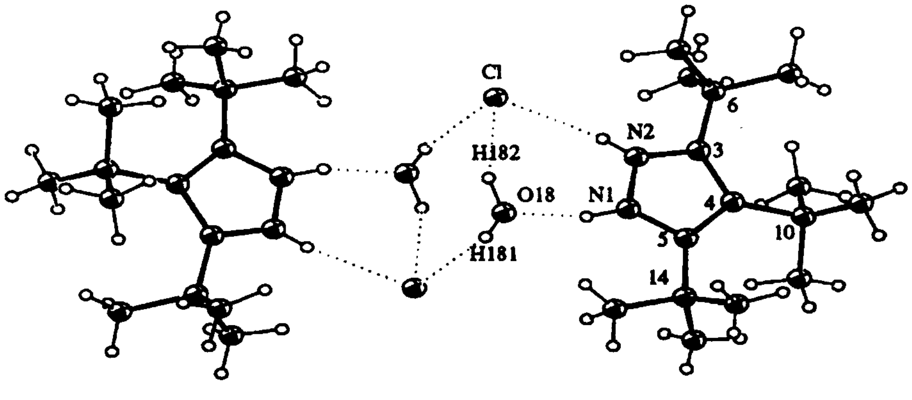

Figure 1. Ortep[15] view of IH^+ showing the atomic numbering. Ellipsoids are drawn at the 30% probability level. For clarity purposes, only one conformation of the disordered *tert*-butyl group has been plotted

Table 4. Geometric parameters (Å, °)

Bond	**IH**$^+$	**II**	**I** (AM1)	**IH**$^+$ (AM1)	**II** (AM1)	**IIH**$^+$ (AM1)
N-1–N-2	1·340(4)	1·333(2)	1·316	1·345	1·339	1·360
N-1–C-5	1·345(4)	1·412(2)	1·405	1·396	1·436	1·424
N-2–C-3	1·323(4)	1·333(2)	1·369	1·397	1·357	1·379
C-3–C-4	1·421(5)	1·412(2)	1·475	1·449	1·473	1·449
C-4–C-5	1·421(4)	1·412(2)	1·428	1·449	1·424	1·443
N-1–C-6	—	1·529(2)	—	—	1·497	1·520
C-3–C-6/C-6′	1·545(6)	1·529(2)	1·514	1·518	1·511	1·516
C-4–C-10/C-7′	1·555(6)	1·554(2)	1·496	1·501	1·495	1·500
C-5–C-14/C-7	1·534(5)	1·554(2)	1·509	1·518	1·510	1·517
N-1–N-2–C-3	111·0(3)	108·7(1)	107·9	109·9	109·7	112·6
N-2–C-3–C-4	107·1(3)	110·1(1)	108·8	106·7	108·7	106·2
C-3–C-4–C-5	105·4(3)	105·3(1)	104·4	105·5	104·2	105·2
N-1–C-5–C-5	107·0(3)	105·3(1)	105·4	107·0	106·2	107·8
N-2–N-1–C-5	109·5(3)	110·1(1)	113·4	110·0	109·9	106·5
C-6–N-1–C-5	—	137·8(1)	—	—	126·9	128·1
C-6–N-1–N-2	—	111·3(1)	—	—	116·5	116·6
C-6/C-6′–C-3–C-4	137·9(3)	137·8(1)	134·5	136·7	132·3	134·9
C-6/C-6′–C-3–N-2	115·0(3)	111·3(1)	116·6	116·5	118·6	118·5
C-10/C-7′–C-4–C-5	127·6(3)	128·9(1)	126·9	126·8	127·8	127·8
C-10/C-7′–C-4–C-3	126·8(3)	123·7(1)	128·6	127·7	126·6	125·8
C-14/C-7–C-5–N-1	114·6(3)	123·7(1)	118·0	116·8	122·6	121·5
C-14/C-7–C-5–C-4	138·4(3)	128·9(1)	136·5	136·1	127·6	127·7
N-1–N-2–C-3–C-4	1·0(4)	2·4(2)	2·4	10·2	5·3	6·6
N-2–C-3–C-4–C-5	−1·8(4)	−6·1(2)	−4·7	−7·5	−10·7	−11·6
C-3–C-4–C-5–N-1	1·9(3)	7·2(2)	5·0	2·4	11·6	12·6
N-2–N-1–C-5–C-4	−1·3(4)	−6·1(2)	−4·0	3·9	−9·2	−8·8
C-5–N-1–N-2–C-3	0·2(4)	2·4(2)	1·0	−8·9	2·4	1·4
C-4–C-5–N-1–C-6	—	162·6(2)	—	—	140·7	136·9
C-5–N-1–C-6–C-8	—	105·6(2)	—	—	117·6	119·9
C-5–N-1–C-6–C-9	—	−21·3(3)	—	—	−6·6	−3·5
C-5–N-1–C-6–C-10	—	−137·7(2)	—	—	−124·8	−122·0
N-1–N-2–C-3–C-6/C-6′	−177·6(3)	—	−174·6	−168·1	−167·8	−166·8
N-2–C-3–C-6–C-7	139·3(7)/−25·3(7)	—	137·4	139·2	24·4	24·4
N-2–C-3–C-6–C-8	40·1(6)/−122·6(5)	—	19·2	20·9	−94·6	−95·2
N-2–C-3–C-6–C-9	−82·3(8)/108(1)	—	−97·2	−96·0	141·0	141·1
N-2–C-3–C-4–C-10/C-7′	174·2(3)	—	171·9	170·2	156·6	157·0
C-3–C-4–C-10/C7′–C-11	142·4(4)/−43·5(6)	—	−30·6	−30·5	−30·5	−31·1
C-3–C-4–C-10/C-7′–C-12	39·9(7)/81·8(9)	—	91·8	91·7	91·7	91·0
C-3–C-4–C-10/C-7′–C-13	−93·4(6)/−138·9(6)	—	−146·5	−146·5	−144·8	−145·5
C-3–C-4–C-5–C-14/C-7	−176·0(4)	−156·8(2)	−170·8	−172·7	−147·0	−147·7
N-1–C-5–C-14/C-7–C-15/C-11	−115·3(4)	−141·4(4)	−129·3	−126·4	−132·1	−132·7
N-1–C-5–C-14/C-7–C-16/C-12	119·4(4)	−29·0(2)	106·1	109·0	−18·1	−18·6
N-1–C-5–C-14/C-7–C-17/C-13	3·1(5)	93·7(2)	−12·5	−9·5	105·3	104·7
C-7′–C-4–C-5–C-7	—	39·2(3)	—	—	46·0	44·1

Compound	X–H···Y	X–H	X···Y	H···Y	X–H···Y	Symmetry
IH$^+$	N-2–H-2···Cl	0·79(6)	3·100(4)	2·35(6)	171(6)	*x y z*
IH$^+$	N-1–H-1···O-18	0·92(4)	2·699(5)	1·81(5)	166(4)	*x y z*
IH$^+$	O-18–H-182···Cl	0·90(10)	3·124(5)	2·43(8)	146(6)	*x y z*
IH$^+$	O-18–H-181···Cl	0·79(4)	3·119(4)	2·93(4)	98(3)	−*x* −*y* −*z*

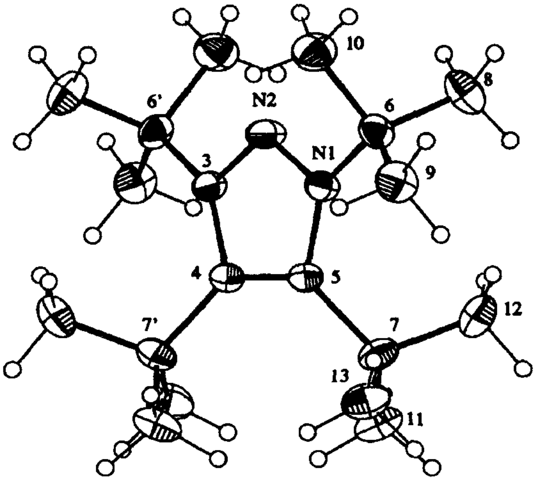

Figure 2. Ortep[15] view of **II** showing the atomic numbering. Ellipsoids are drawn at the 30% probability level

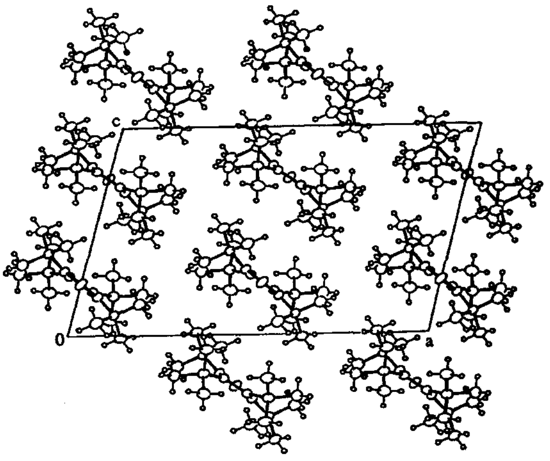

Figure 4. Crystal packing of **II** down the *b* axis

apart, as in 3,5-di-*tert*-butylpyrazole (**III**) and its hydrochloride (**IIIH**$^+$), no deformation was observed in the solid state.[20,21] In **IH**$^+$, the disordered *tert*-butyl groups present approximately 'perpendicular' conformations (30, −90, 150°)[22] which are symmetrically related with regard to the pyrazole plane (−30, 90, −150°) (Table 4). The third group, not disordered, is in a 'parallel' conformation (0, 120, −120°),[21] the C-17 atom being eclipsed with the N-1 atom. In **II**, all groups display the 'perpendicular' conformation.

The lack of planarity of pyrazole rings in **IH**$^+$ and **II** was also supported by semi-empirical AM1 calculations.[23] Although this method overestimates the pyrazole deformation, which is greater in the cations than in the neutral molecules (Table 4), the agreement is fairly good even in the description of the conformation of *tert*-butyl groups and in the external angular distortions observed in the x-ray study. The C_{sp^3} atoms bonded to the pyrazole ring deviate up to 0·25 and to 0·74 Å for **IH**$^+$ and **II**, respectively, with respect to that ring. The greatest discrepancies appeared in the bond distances, larger in the AM1 calculation. Therefore, the loss of planarity of these molecules can be attributed to the proximity of bulky substituents and not to crystal packing effects.

In **IH**$^+$, two water molecules centrosymmetrically related are hydrogen bond bridged by the chlorine anions and the group of $(Cl^- \cdots H_2O)_2$ acts as acceptor of the two N–H hydrogen bonds forming dimers (Table 4 and Figure 1). The geometry of the Cl^- and H_2O arrangement is similar to that reported previously,[21] O···Cl = 3·124(5), 3·119(4) Å and O···Cl···O = 76·9(1)° vs 3·32(7) Å and 78(7)°. The crystal in **IH**$^+$ consists of these discrete units while the molecules in **II** are separated by van der Waals forces. There are no voids in

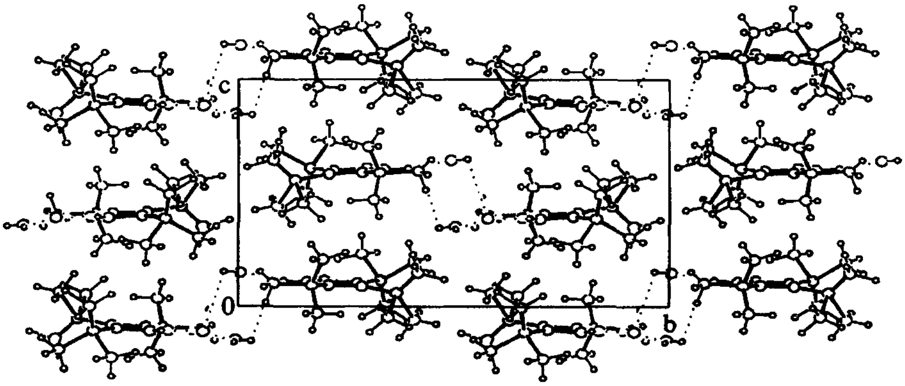

Figure 3. Crystal packing of **IH**$^+$ down the *a* axis

Table 5. AM1 calculation of the proton affinity of pyrazoles (all values in kcal mol^{-1})[a]

Compound	ΔH_f Neutral form	ΔH_f Cation	Calc. *PA*[b]	Exp. *PA*[c]	*PA* calc. by equation (6)
3,4,5-Tri-*tert*-butylpyrazole (**I**)	28·4	179·0	216·6	231·3	228·7
1,3,4,5-Tetra-*tert*-butylpyrazole (**II**)	39·4	180·7	225·9	237·2	237·7
3,5-Di-*tert*-butylpyrazole (**III**)	24·2	177·4	214·0	227·2[d]	226·2
Pyrazole (**IV**)	65·6	229·9	202·9	213·3[d]	215·5
1-*tert*-Butylpyrazole (**V**)	59·4	213·4	213·2	—	225·4
Bent pyrazole (**IVb**)	82·6	250·1	199·7	—	212·4

[a] According to equation (5): $B_{ref}(g) + NH_{4^+}(g) \rightleftharpoons B_{ref}H^+(g) + NH_3(g)$.
[b] $\Delta H_f(H^+) = 367{\cdot}2$ kcal mol^{-1}.[25]
[c] $PA(NH_3) = 204{\cdot}0$ kcal mol^{-1}.
[d] From Ref. 28.

the structures, although the total packing coefficients are rather low, 0·646 and 0·651, respectively; this fact, usually associated with the presence of *tert*-butyl groups,[24] is also reflected in the low density of both compounds. The chlorine anions and water molecules are located in cavities whose corresponding shape, characterized by the planar inertial moments of volume over those of surface, can be described as a torus.[25] The local packing coefficient in **IH**$^+$ is 0·525.

Having demonstrated that the deformations found in the crystal are intrinsic properties, we can return to the problem of the gas-phase basicities and the possible influence of the distortion of aromatic rings on their thermodynamic properties. We have reported that AM1 basicities are well correlated with experimental *PA* values.[26] For 67 compounds the following equation holds:

$$PA(\text{AM1}) = -20{\cdot}36 + 1{\cdot}036(\pm 0{\cdot}028)\ PA(\text{exp}) \quad (6)$$
$$n = 67,\ r^2 = 0{\cdot}965$$

We have gathered in Table 5 the relevant information necessary for the following discussion.

The differences (ΔPA) between **I** and **II** (+9·3 kcal mol^{-1}) and **IV** and **V** (+10·3 kcal mol^{-1}) (1 kcal = 4·184 kJ) are similar, hence the steric effect on the basicity does not seem to be important because the effects largely cancel out. If we add to the value for pyrazole itself (**IV**, $PA = 202{\cdot}9$ kcal mol^{-1}) the effect of *tert*-butyl substituents (calculated from monosubstituted derivatives lacking steric repulsion) from Ref. 24 (position 3, 6·06; position 4, 3·12; position 5, 4·81 kcal mol^{-1}) and position 1 (9·3 kcal mol^{-1}), the resulting value is 226·2 kcal mol^{-1}, close to 225·9 kcal mol^{-1}, another indication of the absence of steric effects between neutral and protonated species.

To approach this problem differently, we carried out a calculation, within the same approximation, for an unsubstituted pyrazole having the ring geometry of compounds **II** and **IIH**$^+$. The result, reported in Table 5 for 'bent pyrazole **IVb**' shows that the neutral molecule is 17·0 kcal mol^{-1} less stable than the planar molecule, whereas the cation (**IVbH**$^+$) is 20·2 kcal mol^{-1} less stable. The fact that the cation loses more energy than the neutral molecule is probably related to the fact that the former is more aromatic than the later (pyrazolium cations have much more regular geometries than pyrazoles; see Table 4 and Refs 20 and 21). However, the difference (20·2 − 17·0 = 3·2 kcal mol^{-1}) is relatively small and, as a consequence, structural distortion only brings about a modest base-weakening effect.

SUPPLEMENTARY MATERIAL

Lists of structure factors, thermal components, hydrogen parameters and bond distances and angles have been deposited at the Cambridge Crystallographic Data Centre.

ACKNOWLEDGEMENTS

Financial support was provided by the Spanish DGICYT (PB93-0125 and PB93-0289-C02-02) and by the EU (CHRX-CT94-0582).

REFERENCES

1. O. Ermer, *Angew. Chem., Int. Ed. Engl.* **26**, 782–784 (1987).
2. G. G. Hall, *J. Chem. Soc., Perkin Trans. 2* 1491–1492 (1993).
3. L. Carballeira, J. Casado, E. González and M. A. Rios, *J. Chem. Phys.* **77**, 5655–5663 (1982).
4. J. E. Rice, T. J. Lee, R. B. Remington, W. D. Allen, D. A. Clabo and H. F. Schaeffer, *J. Am. Chem. Soc.* **109**, 2902–2909 (1987).
5. D. M. Collard, M. J. Sadri, D. VanDerveer and K. S. Hagen, *J. Chem. Soc., Chem. Commun.* 1357 (1995), and references cited therein.
6. A. W. Krebs, E. Franken, M. Müller, H. Colberg, W. Cholcha, J. Wilken, J. Ohrenberg, R. Albrecht and E. Weiss, *Tetrahedron Lett.* **33**, 5947–5950 (1992).

7. H.-H. Büker and H.-F. Grützmacher, *Int. J. Mass. Spectrom. Ion Processes* **109**, 95–104 (1991).
8. R. Houriet and E. Rolli, *New J. Chem.* **11**, 221–224 (1987).
9. A. T. Lehman, M. M. Bursey, *Ion Cyclotron Resonance Spectrometry*. Wiley, New York (1976); M. V. Buchanan (Ed.), *Fourier Transform Mass Spectrometry, Evolution, Innovation and Applications*. ACS Symposium Series, No. 359, American Chemical Society, Washington, DC (1987); K. R. Jennings (Ed.), *Fundamentals of Gas Phase Ion Chemistry*. NATO ASI Series, Vol. 347, Kluwer, Dordrecht (1991).
10. (a) J.-L. M. Abboud, R. Notario, E. Ballesteros, M. Herreros, O. Mó, M. Yáñez, J. Elguero, G. Boyer and R. M. Claramunt, *J. Am. Chem. Soc.* **116**, 2486–2492 (1994); (b) J.-L. M. Abboud, O. Mó, J. L. G. de Paz, M. Yáñez, M. Essefar, W. Bouab, M. El-Mouhtadi, R. Mokhlisse, E. Ballesteros, M. Herreros, H. Homan, C. López-Mardomingo and R. Notario, *J. Am. Chem. Soc.* **115**, 12468–12476 (1993).
11. (a) S. G. Lias, J. F. Liebman and R. D. Levin, *J. Phys. Chem. Ref. Data* **13**, 695 (1984); (b) J. E. Szulejko and T. B. McMahon, *J. Am. Chem. Soc.* **115**, 7839–7848 (1993).
12. R. Notario, M. Herreros, A. El Hammadi, H. Homan, J.-L. M. Abboud, I. Forfar, R. M. Claramunt and J. Elguero, *J. Phys. Org. Chem.* **7**, 657–662 (1994).
13. A. Altomare, M. C. Burla, M. Camalli, G. Cascarano, C. Giacovazzo, A. Guagliardi and G. Polidori, *J. Appl. Crystallogr.* **27**, 435 (1994).
14. *International Tables for X-Ray Crystallography*, Vol. IV. Kynoch Press, Birmingham (1974).
15. S. R. Hall and J. M. Stewart, *XTAL 3.0*, Universities of Western Australia and Maryland, Perth (1990).
16. M. Martínez-Ripoll and F. H. Cano, *PESOS*, unpublished program.
17. M. Nardelli, *Comput. Chem.* **7**, 95–98 (1983).
18. D. Cremer and J. A. Pople, *J. Am. Chem. Soc.* **97**, 1354–1358 (1975).
19. F. H. Allen, O. Kennard, D. G. Watson, L. Brammer, A. G. Orpen and R. Taylor, *J. Chem. Soc., Perkin Trans. 2* S1–S19 (1981).
20. A. L. Llamas-Saiz, C. Foces-Foces, F. H. Cano, P. Jiménez, J. Laynez, W. Meutermans, J. Elguero, H.-H. Limbach and F. Aguilar-Parrilla, *Acta Crystallogr., Sect. B* **50**, 746–762 (1994).
21. C. Fernández-Castaño, C. Foces-Foces, N. Jagerovic and J. Elguero, *J. Mol. Struct.* **335**, 265–271 (1995).
22. P. Molina, M. Alajarín, C. López Leonardo, R. M. Claramunt, C. Foces-Foces, F. H. Cano, J. Catalán, J. L. G. de Paz and J. Elguero, *J. Am. Chem. Soc.* **111**, 355–363 (1989).
23. J. J. Stewart, *MOPAC 6.0*. Frank J. Seiler Research Laboratory, USAF Academy, CO (1990).
24. I. Alkorta, I. Rozas, J. Elguero, C. Foces-Foces and F. H. Cano, unpublished results.
25. F. H. Cano and M. Martínez-Ripoll, *J. Mol. Struct. (Theochem)* **258**, 139–158 (1992).
26. A. El Hammadi, M. El Mouhtadi, R. Notario, J.-L. M.Abboud and J. Elguero, *J. Chem. Res. (S)* 172–173, *(M)* 1080–1096 (1995).
27. S. G. Lias, J. E. Bartmess, J. L. Holmes, R. D. Levin, J. F. Liebman and W. G. Mallard, *NIST Reference Database 19A, Standard Reference Data*. Computerized Version 1.1, NIST, Gaithersburg, MD (1989).
28. J.-L. M. Abboud, P. Cabildo, T. Cañada, J. Catalán, R. M. Claramunt, J. L. G. de Paz, J. Elguero, H. Homan, R. Notario, C. Toiron and G. I. Yranzo, *J. Org. Chem.* **57**, 3938–3946 (1992).